

**CHARACTERIZATION OF ALUMINUM NITRIDE THIN FILMS  
FOR MICRO AND NANOMECHANICAL RESONATORS**

By

Diego Andrés Aponte-Roa

A thesis submitted in partial fulfillment of the requirements for the degree of

MASTER OF ENGINEERING

in

ELECTRICAL ENGINEERING

UNIVERSITY OF PUERTO RICO  
MAYAGÜEZ CAMPUS

2008

Approved by:

---

Rafael A. Rodríguez Solís, Ph.D  
Member, Graduate Committee

---

Date

---

Felix E. Fernández, Ph.D  
Member, Graduate Committee

---

Date

---

Nelson Sepulveda Alancastro, Ph.D  
President, Graduate Committee

---

Date

---

Agnes M. Padovani, Ph.D  
Representative of Graduate Studies

---

Date

---

Isidoro Couvertier, Ph.D  
Chairperson of the Department

---

Date

Abstract of Dissertation Presented to the Graduate School  
of the University of Puerto Rico in Partial Fulfillment of the  
Requirements for the Degree of Master of Engineering

**CHARACTERIZATION OF ALUMINUM NITRIDE THIN FILMS  
FOR MICRO AND NANOMECHANICAL RESONATORS**

By

Diego Andrés Aponte-Roa

2008

Chair: Nelson Sepulveda Alancastro

Major Department: Electrical and Computer Engineering

This work presents the setup of a Physical Vapor Deposition by pulsed DC sputtering system and the characterization of aluminum nitride thin films deposited using the assembled system. The different parts of the system are shown and explained in detail. Deposition of aluminum nitride thin films with thicknesses in the range of 55 to 450nm was done at 500 °C over sapphire (c-cut), glass, silicon  $\langle 1\ 1\ 1 \rangle$ , and silicon  $\langle 1\ 0\ 0 \rangle$  substrates in the Physical Vapor Deposition system. X-ray diffraction and Atomic Force Microscopy were used for the characterization of the aluminum nitride films. Film orientation was found to be related to the deposition pressure. The lowest grain size obtained was 40nm.

Resumen de Disertación Presentado a Escuela Graduada  
de la Universidad de Puerto Rico como requisito parcial de los  
Requerimientos para el grado de Maestría en Ingeniería

**CHARACTERIZATION OF ALUMINUM NITRIDE THIN FILMS  
FOR MICRO AND NANOMECHANICAL RESONATORS**

Por

Diego Andrés Aponte-Roa

2008

Consejero: Nelson Sepulveda Alancastro  
Departamento: Ingeniería Eléctrica y Computadoras

Este trabajo presenta el ensamblaje de un sistema de deposición física de vapor de pulverización catódica por DC pulsado y la caracterización de películas delgadas de nitruro de aluminio depositadas usando dicho sistema. Todas las partes del sistema son mostradas y explicadas en detalle. Se depositaron películas delgadas de nitruro de aluminio con un grosor desde 55 hasta 450nm a 500 °C sobre sustratos de zafiro (corte-c), vidrio, silicio  $\langle 1\ 1\ 1 \rangle$  y silicio  $\langle 1\ 0\ 0 \rangle$  en el sistema de deposición física de vapor. Difracción de rayos X y el Microscopio de Fuerza Atómica fueron usados para caracterizar las películas de nitruro de aluminio. Una relación entre la presión de deposición y la orientación de la película fue encontrada. El tamaño del grano más pequeño obtenido fue 40nm.

To my brothers Jorge and Carlos, for all the unconditional love, motivation and support in all my career. To my father Alberto Aponte, in loving memory.

To Beatriz Roa...

My light, my guide, my teacher, my sun, my world..... my mother!

## ACKNOWLEDGMENTS

I would like to express my gratitude to my advisor, Dr. Nelson Sepulveda-Alancastro for his continuous support, dedication and help in this project, and to be patient in the process of writing this document. Also, I would like to thank my graduate committee formed by Dr. Felix E. Fernández and Rafael A. Solís for their contributions to my work.

I would also like to thank Professors Rogerio Palomera and Gladys Omayra Ducoudray for helping me in different situations during this master's degree. I want acknowledge my friends who are close to my work: Edgar, Alix, Pablo Lozada, Diego Arias, Rasputin and CS members, and especially to Luis Quintero and Fabian Benitez. To my housemates in Puerto Rico (almost my family) Elkin, David, Constanza and Camilita. To Sandy for her continuous support, and to the INEL/ICOM department for giving me the opportunity to study at this prestigious University. To Yari for her support and love, and for encouraging me to finish this research.

This project has been supported by the NSF-PR-EPSCoR Start-Up funds.

## TABLE OF CONTENTS

	<u>page</u>
ABSTRACT ENGLISH . . . . .	ii
ABSTRACT SPANISH . . . . .	iii
ACKNOWLEDGMENTS . . . . .	v
LIST OF TABLES . . . . .	vii
LIST OF FIGURES . . . . .	viii
1 INTRODUCTION . . . . .	1
1.1 Objectives . . . . .	3
1.1.1 General Objective . . . . .	3
1.1.2 Specific Objectives . . . . .	3
1.2 Thesis Overview . . . . .	3
2 BACKGROUND . . . . .	5
2.1 Introduction . . . . .	5
2.2 AlN Material . . . . .	5
2.3 AlN for MEMS . . . . .	6
2.4 Temperature Dependence . . . . .	9
2.5 PVD of AlN films . . . . .	10
3 PVD SYSTEM . . . . .	13
3.1 Introduction . . . . .	13
3.2 Components of the PVD system . . . . .	14
4 EXPERIMENTAL RESULTS . . . . .	19
4.1 Introduction . . . . .	19
4.2 Deposition and Characterization of AlN thin films . . . . .	20
4.3 Comparison of Results . . . . .	28
5 CONCLUSIONS AND FUTURE WORK . . . . .	31
5.1 Conclusions . . . . .	31
5.2 Future work . . . . .	32

## LIST OF TABLES

<u>Table</u>		<u>page</u>
2.1	Properties of AlN. . . . .	6
2.2	Initial experimental conditions. . . . .	12
3.1	Specifications of the heater. . . . .	16
3.2	Specifications of the sputtering gun. . . . .	16
4.1	AlN thin film on silicon $\langle 1\ 1\ 1 \rangle$ substrate. . . . .	21
4.2	AlN thin film on glass substrate. . . . .	26
4.3	AlN film growth parameters. . . . .	29

## LIST OF FIGURES

<u>Figure</u>	<u>page</u>
2.1 Schematic diagram of the sputtering system. . . . .	11
3.1 PVD System. . . . .	13
3.2 Cryogenics . . . . .	14
3.3 Vacuum Chamber . . . . .	15
3.4 Heater. . . . .	15
3.5 Sputtering Gun. . . . .	17
3.6 Controllers . . . . .	18
4.1 Target wave form at 100 kHz, 80% of duty cycle. . . . .	20
4.2 XRD with grazing angle 3° of AlN thin film on silicon <1 1 1> substrate. . . . .	22
4.3 AFM of AlN thin film on silicon <1 1 1> substrate. . . . .	22
4.4 XRD of AlN thin film on sapphire (c-cut) substrate. . . . .	23
4.5 XRD of AlN thin film on silicon <1 0 0> substrate. . . . .	24
4.6 AFM of AlN thin film on silicon <1 0 0> substrate. . . . .	25
4.7 XRD with grazing angle 3° of AlN thin film on glass substrate. . . . .	26
4.8 XRD of AlN thin film on silicon <1 0 0> substrate. . . . .	27
4.9 AFM of AlN thin film on silicon <1 0 0> substrate with varying thickness . . . . .	28

# CHAPTER 1

## INTRODUCTION

RF Microelectromechanical systems (MEMS) are one of the major MEMS businesses in the electronics industry with applications that can impact a broad spectrum of areas, including telecommunications, radars, antennas and wireless applications. Nanoelectromechanical systems (NEMS) technologies are used to fabricate sensors and actuators at the nanometer scale. It is an important branch of applications in nanotechnology in which the control of matter for device fabrication on a scale below 100 nm is studied.

RF MEMS/NEMS will create innovative ways to change the current RF systems. Particularly, an area of current research focus is the implementation of resonators with a good performance (high Q factor, low motional resistance, low power consumption, etc.). MEMS resonators are used in sensor applications [1, 2] and in wireless communication [3], where they can be used as filters (due to their frequency selectivity property), oscillators and mixers.

In recent years, research efforts have focused on the implementation of sensor applications using NEMS resonators. Two novel methods were presented by Aubin et al.[4] to create microfluidic encapsulated NEMS resonator arrays. They used a silicon nitride NEMS resonators that showed high resonance frequency and quality factor. This work demonstrated that biosensor applications could be done using NEMS devices.

An oscillator consists of a resonator in connection with a feedback amplifier, where its output signal has the resonant frequency of the resonator. Oscillators have many electronic applications, such as clocks, synchronization circuits, and high frequency carriers with stable and repetitive waveforms necessary for application in some modern wireless communication systems.

A mixer has two or more input signals and the output signal is the sum of the input signals. Some years ago, Artur Erbe and Robert Blick [5] reported a mechanical mixer in the radio-frequency regime employing the nonlinear response of a strongly-driven nanomechanical resonator. This opened up a wide range of applications, particularly for signal processing. Two years later, the same research group presented a nanomechanical resonator with an operating frequency in the range of several 100 MHz [6]. These resonators can be used for novel structures in mechanical mixing of high-frequency signal processing and as very sensitive detectors, or frequency selective components in electronic communication systems.

RF-filters are of great interest for mobile technology because they can protect the sensitive receiver path from interference and noise from various RF sources. Actually, Surface Acoustic Wave (SAW) filters or ceramic filters are used in most phones. Nevertheless, ceramic filters are expensive and too big for future mobile phones, therefore are likely to disappear as soon as an alternative technology becomes available. On the other hand, Bulk Acoustic Wave (BAW) filters could replace conventional RF-filters because they have demonstrated good performance, size advantages and very low cost [7].

Some materials and particular structures have been investigated for MEMS resonator applications and each one of them has shown different performance and properties. Aluminum nitride (AlN) is a material of great interest for different MEMS applications due to its mechanical and piezoelectric properties. This material

is able to provide the high frequency and Q values necessary for communication systems with high performance, low-cost, low-power, high reliability and small-size components. Furthermore, it can sustain very high temperatures without changing its properties substantially, which makes it very attractive for harsh environment applications.

A Physical Vapor Deposition (PVD) system has been assembled for the deposition of AlN thin films. The deposited AlN thin films were characterized using X-ray diffraction (XRD) and Atomic Force Microscopy (AFM).

## **1.1 Objectives**

### **1.1.1 General Objective**

To assemble a PVD system for the deposition of AlN thin films and characterize the deposited films.

### **1.1.2 Specific Objectives**

- Setup of the PVD by pulsed DC sputtering system for AlN thin films.
- Deposition of AlN thin films over sapphire on c-cut, glass, silicon  $\langle 1\ 1\ 1 \rangle$ , and silicon  $\langle 1\ 0\ 0 \rangle$  substrates.
- Characterization of AlN thin films using XRD and AFM.

## **1.2 Thesis Overview**

This thesis presents the assembly process of a PVD system by pulsed DC sputtering for AlN thin film deposition and the characterization of these films. Chapter 2 discusses the AlN material and explains why it is so important for MEMS applications. It also discusses the different techniques for fabrication of thin films, focusing on the PVD technique.

The third chapter of this thesis talks about the deposition system setup. All the parts of this PVD by sputtering system are shown and explained in detail. The system is located at the Physics building of the University of Puerto Rico - Mayaguez Campus, under supervision of Dr. Felix Fernández.

The fourth chapter describes the recipes used during the experimentations. XRD and AFM analysis are presented for some samples. A comparison of results for the samples in different substrates is also shown. Chapter 5 presents the conclusions of this work and future research recommendations.

# CHAPTER 2

## BACKGROUND

### 2.1 Introduction

This chapter presents a summary of the latest results obtained in MEMS applications in a broad spectrum of areas, particularly in MEMS resonators. The justification for using AlN and some of the common techniques used for the fabrication of these films are discussed.

### 2.2 AlN Material

Aluminum nitride is one of the most versatile III-V compounds. It has a hexagonal crystal structure and is a covalently-bonded material. AlN possesses a large energy band-gap of about 6 eV [8, 9], high thermal conductivity [260W/(m.K)], high breakdown voltage (15 kV/mm), high resistivity ( $10^{14}\Omega\cdot\text{cm}$ ), and good thermal expansion coefficient. This material is stable to very high temperatures in inert atmospheres, but in air, surface oxidation occurs above 700°C. Above this temperature, a layer of aluminum oxide protects the material up to 1370°C, at which bulk oxidation occurs. Also, this material keeps its mechanical and piezoelectric properties at temperatures above 1000°C [10, 11].

These interesting and reproducible properties convert the AlN as a commercially viable product and one of the materials of most interest in MEMS research. Several authors have focused on properties of AlN thin films for electronics, opto-electronics, and acoustic applications. For example, Spina et al.[12] suggested that the AlN is

a candidate to be used as a heat spreader in silicon integration processes due its good dielectric and thermal properties. Two years later, applications of AlN layers as heat spreaders were examined in NPN-BJT in a variety of configurations by the same research group mentioned above [13].

Table 2.1 shows properties of AlN that have been studied for MEMS applications.

Table 2.1: Properties of AlN.

<b>Property / Material</b>	<b>AlN</b>
Density	3260kg/m <sup>3</sup>
Young's modulus	330GPa
Thermal conductivity	260W/(m*K)
Volume resistivity	10 <sup>14</sup> Ω*cm
Thermal expansion coefficient	4.5*10 <sup>-6</sup> /°C
Poisson's ratio	0.24

### 2.3 AlN for MEMS

AlN is a material that presents good mechanical and piezoelectric properties. It is extensively used in RF MEMS micro-machined resonators and filters devices due to its high resistivity and piezoelectric coefficient, which is the largest among nitrides, and also because it can be patterned using conventional photolithographic techniques. Since the resonator behavior depends greatly on the structural material, the performance of AlN resonators has potential applications in MEMS-based tunable filters and oscillators for wireless applications.

The demand of radio-frequency (RF) filters and frequency reference elements has focused attention on the reduction of size, power consumption, high frequencies, and high quality factors (Qs). Also, issues related to price and consumer availability have pushed current research interests towards the manufacturing of a single-chip integrated RF solution. In order to accomplish higher frequencies and Q values, polycrystalline diamond has been explored as a new MEMS resonator material that

can replace the polycrystalline silicon RF MEMS resonators [14]. This material is extremely wear resistant, showed highest Qs on polycrystalline material, and has an intrinsically hydrophobic surface. Nevertheless, AlN MEMS contour mode resonator technology has the advantage of combining low motional resistance and high Qs with the ability to define multiple frequencies on the same substrate. This could enable the fabrication of arrays of microresonators with different frequencies on a single chip.

Gianluca Piazza and Albert P. Pisano [15] reported the experimental results on a new class of contour-mode aluminum nitride resonators. Their work showed high Qs in vacuum and air, and low motional resistance for frequency range from 23 MHz to 225 MHz. Circular and rectangular plates were used. These rectangular plate resonators offer advantages in terms of size reduction compared to commercially available piezoceramics used for Very High Frequency (VHF range from 30 MHz to 300 MHz) applications while maintaining the same Qs.

A year later, the technology was extended by the same research group mentioned above to Ultra High Frequency (UHF range from 300 MHz to 3 GHz) [16]. Their work showed experimental results on a new class of ring-shaped with high quality factors in air and low motional resistance for frequencies ranging from 233 MHz to 656 MHz. They obtained center frequencies that can be lithographically tuned.

Optical lithography permits the co-fabrication of multiple filters at arbitrary frequencies on the same chip for both electrostatic and piezoelectric transducer devices. The main problem is that the electrostatic RF resonators suffer from high motional resistance that prevent their interface with  $50\Omega$  systems. Whereas, for the piezoelectric devices, the use of contour modes (with frequencies determined by in-plane dimensions) permits the batch fabrication of arrays of piezoelectric microresonators with different frequencies on a single chip. That technology could

replace the existent technology (Film Bulk Acoustic Resonator (FBAR) and shear-mode quartz resonators), which does not permit the manufacturing of a single-chip RF module because frequency selective arrays of piezoelectric resonators cannot be fabricated on the same substrate, since film thickness sets frequency.

Recent advances have verified that AlN contour-mode resonators are the unique structures capable of offering high quality factors in air and spanning frequency from 10 MHz to 3 GHz (in their fundamental mode of operation) on the same silicon chip. They have also demonstrated impedance values that can be matched to  $50\Omega$  RF systems. Initial experimental results were reported by Piazza et al.[17] using these devices for circuit application such as band pass filtering and frequency synthesis. In addition, the most significant experimental results that were obtained by Stephanou et al.[18, 19] were presented by making arrays of these resonators.

Gianluca Piazza, Philip J. Stephanou, and Albert Pisano [20] reported in December of 2006 a new class of rectangular plate and ring-shaped structures that improved the quality factor in air. The actuation/detection method for these devices is using piezoelectric testing, by making the devices operate in a radial contour mode. This method and the electrostatic testing method for RF MEMS resonators were explained by Sepulveda et al.[21].

A few months later, the technology was extended by the same research group [20] and the experimental results on a new class of single-chip multiple-frequency filters were presented [22]. These structures were made out of an aluminum nitride layer sandwiched between a bottom platinum electrode and a top aluminum electrode. They obtained filters with low motional resistance that can have direct interface with standard  $50\Omega$  systems. It is worth mentioning that all of the above AlN application studies were focused on the application itself and not on the material characterization.

## 2.4 Temperature Dependence

In the micromechanical resonator device design, the temperature dependence of the materials' elastic properties is an important factor at the time of determining the device reliability. The temperature effects on the elastic properties of Si thin films using an electrostatic micromechanical resonator in the range of 25 to 600° Celsius were studied by Jeong et al.[23]. They estimated the elastic modulus of pure Si using a short-dwell-time experiment, in which data at various temperatures were measured independently from each specimen. Twenty-minute dwell time data was also measured for the comparison with the non-oxidized data (pure Si). This work showed the following polynomial fitting equation for the elastic modulus of Si that is only valid in the range of room temperature to 600°C:

$$E_{Si}(T) = 167.98 * 10^9 - 1.167 * 10^7 T + 1757.9T^2 [Pa] \quad (2.1)$$

Where  $T$  is temperature in Celsius. In a similar way, the Young's modulus temperature dependence of VO<sub>2</sub> thin films in the temperature range of 30 to 90°C was presented by Sepulveda et al.[24] by measuring the resonant frequency of the VO<sub>2</sub> coated Si cantilevers using a light scattering system. The resonant frequency of a coated cantilever beam, where the coating is much thinner than the uncoated cantilever, is given by:

$$f_c^2 = K \frac{\left\{ E_1(wt/12) + E_2\delta \left[ (w + 2\delta) \left( \frac{1}{2} + \frac{\delta}{t} + \frac{\delta^2}{2t^2} \right) + \frac{t}{6} \right] \right\}}{\rho_1 tw + 2\rho_2\delta(w + t + 2\delta)} [Hz], \quad (2.2)$$

where  $l$ ,  $t$ ,  $w$ ,  $\rho_1$ , and  $E_1$  are the length, thickness, width, density, and Young's modulus of the uncoated cantilever, respectively.  $E_2$ ,  $\delta$ , and  $\rho_2$  are the elastic modulus, thickness, and density of the coating, respectively, and  $K$  was previously defined as:  $K = \frac{12.36t^2}{(2\pi)^2 l^4}$  by Bishop and Johnson [25]. The Young's modulus of VO<sub>2</sub> was calculated by combining it with the commonly-known equation used for calculating the resonant frequency of an uncoated cantilever beam:

$$f_u = \frac{1.02t}{2\pi l^2} \sqrt{\frac{E_1}{\rho_1}} [Hz], \quad (2.3)$$

where  $l$ ,  $t$ ,  $E_1$ , and  $\rho_1$  are the cantilever's length, thickness, Young's modulus, and density, respectively. The combination leads to the following ratio of resonant frequencies:

$$\frac{f_c^2}{f_u^2} = \rho_1 \frac{\left\{ wt + 12 \left( \frac{E_2}{E_1} \right) \delta \left[ (w + 2\delta) \left( \frac{1}{2} + \frac{\delta}{t} + \frac{\delta^2}{2t^2} \right) + \frac{t}{6} \right] \right\}}{\rho_1 tw + 2\rho_2 \delta (w + t + 2\delta)} [Hz], \quad (2.4)$$

where the only variable left in Equation 2.4 is the Young's modulus of the coating ( $E_2$ ). Therefore, the mechanical properties of the deposited AlN films in this work can be calculated using this method.

## 2.5 PVD of AlN films

In the PVD technique, the material to be deposited is converted into vapor by physical means. Next, the vapor is transported across a region of low pressure from its source to the substrate to form the thin film. This generally involves plasma (DC, RF, or microwave) activation.

There are several techniques for the deposition of AlN or  $Al_2O_3$  including gas source molecular beam epitaxy, reactive molecular beam deposition (RMBD), chemical vapor deposition (CVD), PVD, etc. PVD is widely used due to the advantage to deposit films at relatively low temperatures when compared with other techniques, such as CVD. This is an advantage because the deposition technique is compatible with most CMOS technologies. PVD by sputtering is a technique where atoms or molecules are ejected from a target material by high-energy particle bombardment so that the ejected atoms or molecules can condense on a substrate as a thin film.

Recent investigations recommended a pulsed dc sputtering technique due to its high deposition rates and high quality films. This technique combines the advantages of dc and radio frequency sputtering, solving the charging problem at the target. The pulsing parameters effects were presented by Belkind et al.[26] and the fabrication process for

aluminum nitride thin films by pulsed dc power sputter has also been described in the past [27, 28].

The mechanical, electrical, and optical properties of AlN films deposited by reactive DC pulsed magnetron sputtering on silicon and fused quartz substrates were presented by Mortet et al.[29]. Similarly, the structural, optical, and mechanical properties of aluminium nitride films prepared by reactive DC magnetron sputtering were showed by Venkatara et al.[30]. For both cases, the deposited AlN thin films were characterized using XRD and AFM, as it was also done for the AlN films deposited in this work.

A general schematic of our system is shown in Figure 2.1. When the sample is ready for AlN deposition, it is loaded into the chamber together with the pure Al target and taken to a low pressure level. A mixture of gases is then introduced into the chamber (the total gas flow was maintained using mass flow controllers) and the energy, provided by a Pulse-DC power supply, helps to create the suitable conditions inside the chamber for light-up the plasma.

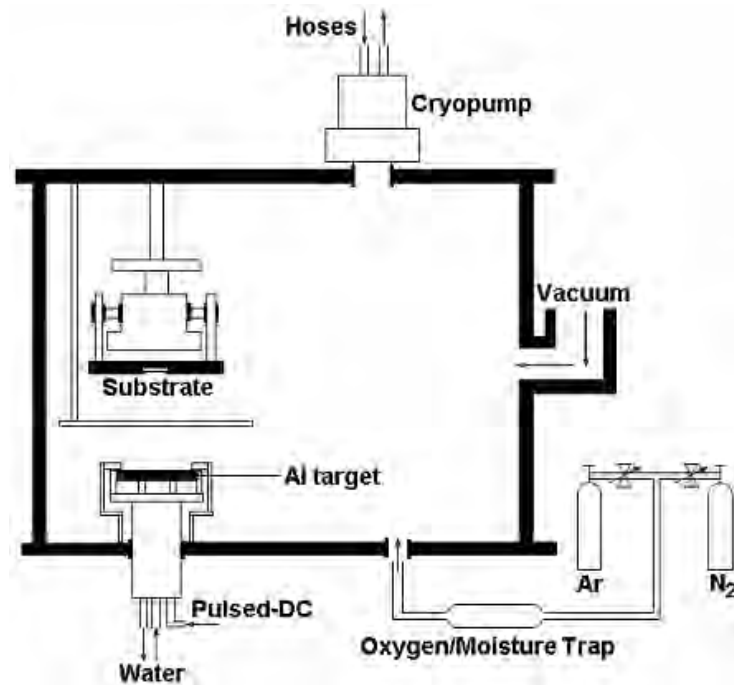


Figure 2.1: Schematic diagram of the sputtering system.

The experimental conditions for asymmetric bipolar pulsed dc sputtering mentioned by Lee et al.[27] were used for starting our experimentation. Table 2.2 shows these conditions.

Table 2.2: Initial experimental conditions.

<b>Parameter</b>	<b>Value</b>
Distance between target and substrate	3in.
Substrate	Si (1 0 0)
Sputtering pressure	3.733Pa
N <sub>2</sub> gas %	70%
Deposition temperature	500 °C
Target current	2.0A
Frequency	100kHz
Duty cycle	80%
Deposition time	90min

# CHAPTER 3

## PVD SYSTEM

### 3.1 Introduction

The work reported in this thesis focuses on the use of aluminum nitride as a micromechanical resonator structural material. This chapter discusses the AlN deposition system. The system setup was done under the supervision of Dr. Felix Fernández. A general photo of the deposition system used is shown in Figure 3.1.

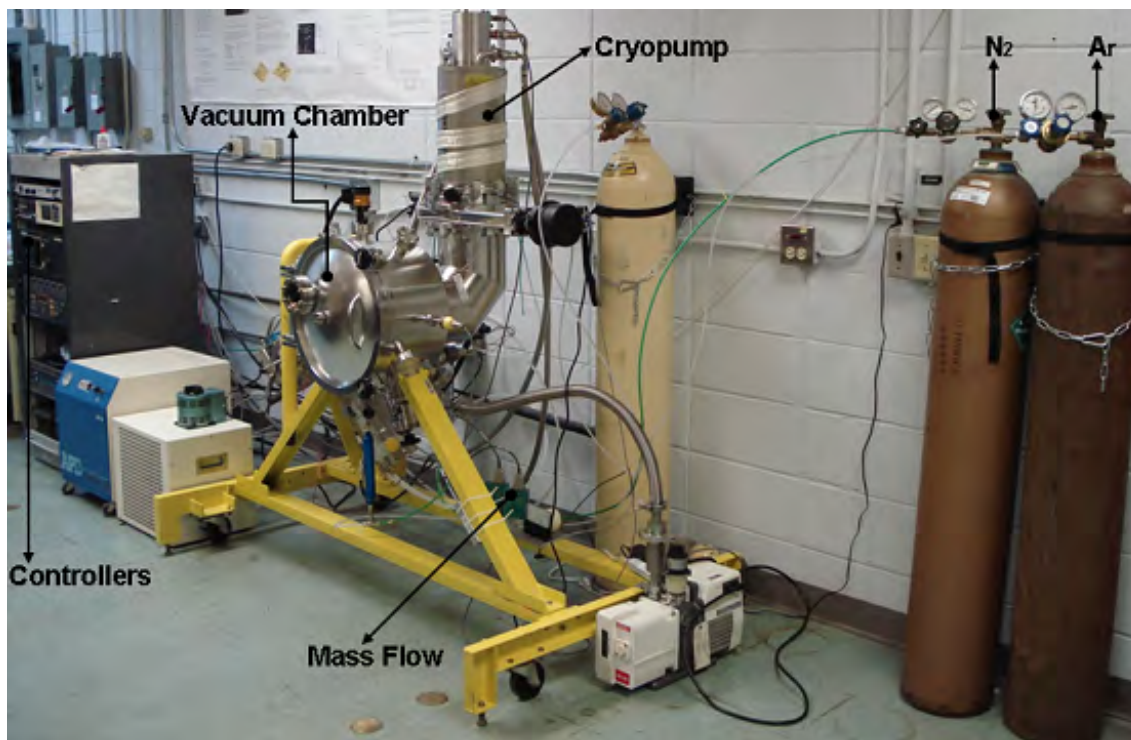


Figure 3.1: PVD System.

### 3.2 Components of the PVD system

The PVD by sputtering system can be divided into 3 parts: cryopump, vacuum chamber, and controllers.

#### A) Cryopump:

A cryopump is a vacuum pump that captures and retains gases and vapors from within a vacuum chamber by condensing them on a very cold surface. The chamber is cooled down and maintained at very low temperatures with liquid helium.

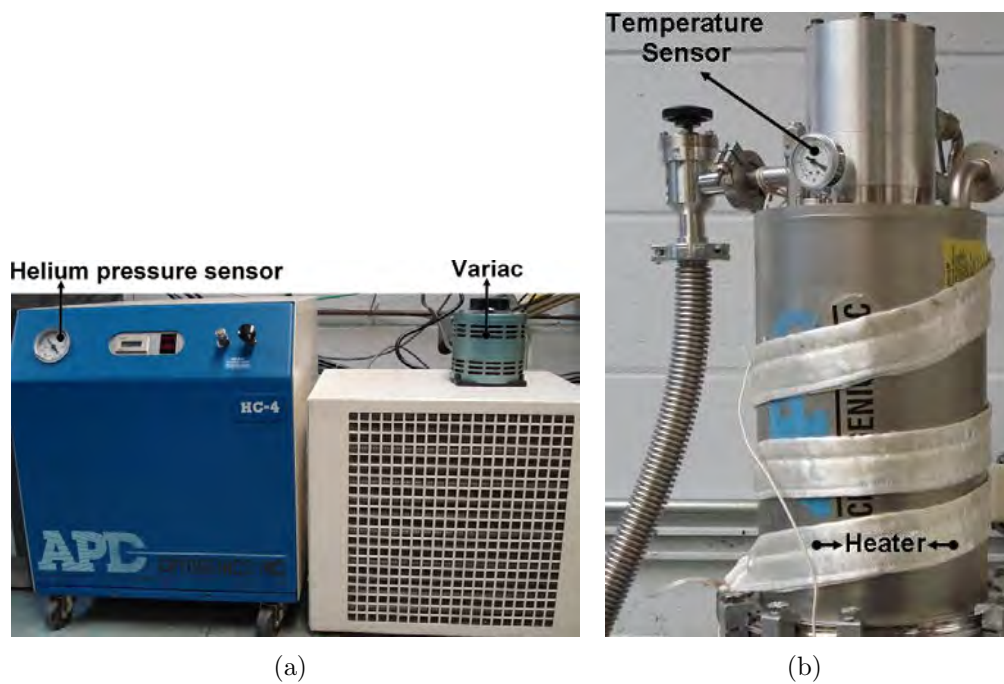


Figure 3.2: Cryopump: (a) Helium Compressor; (b) Cryogenics pump.

An electrical heater was used for pump surface regeneration. Figure 3.2 shows the cryopump system in which a variac was used to control the temperature of the electrical heater. A cryogenic system must also have both helium pressure and temperature sensors. Before starting the compressor, at room temperature, the pressure gauge should indicate 240-245 psig. When the compressor is turned on, the helium pressure sensor needs to be between 300-320 psig for normal operation.

## B) Vacuum Chamber:

A vacuum chamber is a rigid enclosure from which air and other gases are removed by a vacuum pump. Figure 3.3 shows our vacuum chamber. Each one of its inside components will be discussed.

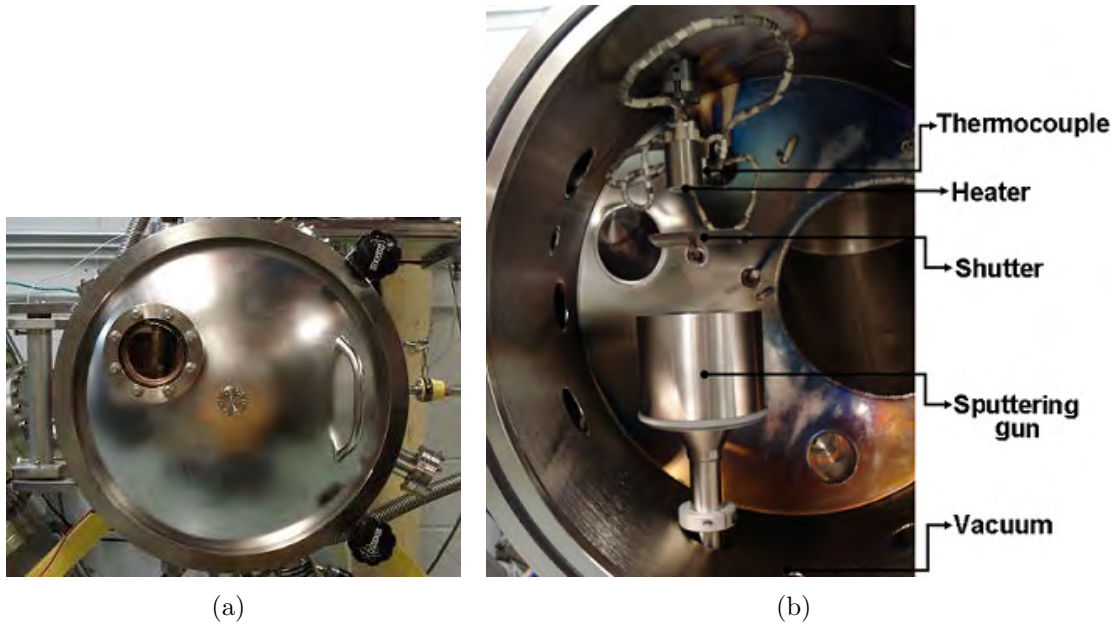


Figure 3.3: Vacuum Chamber: (a) Front-view; (b) Inside-view.

- *Heater:*

The substrate was placed on a UHV button heater (model X-369, Heatwave Inc) for AlN deposition. Figure 3.4 shows the heater used. This heater must be operated in high vacuum.



Figure 3.4: Heater.

A thermocouple is needed for measuring the real temperature at the substrate. The substrate temperature was controlled using the temperature controller shown in Figure 3.6(b). The main heater's specifications are shown in the Table 3.1.

Table 3.1: Specifications of the heater.

Max. Wattage	900 °C			1000 °C		
	Volts	Amps	Watts	Volts	Amps	Watts
190	8.50	5.80	49.0	10.90	6.60	73.0

The deposition temperature was achieved when 8.5 volts were applied to the heater. Since this voltage is close to the heater's limit (10.9V), it is important to control this voltage precisely. This control was also done using the temperature controller.

- *Sputtering Gun:*

Table 3.2 shows the main specifications of the sputtering gun used.

Table 3.2: Specifications of the sputtering gun.

Specification	Value
Maximum sputtering power	1000W DC or 600W RF
Flow rate	5 gallons/minute
Maximum temperature	100 °C
Magnetic enhancement	Permanent

The sputtering gun must be refrigerated up to its operation temperature ( $\sim 50^\circ\text{C}$ ). This is very important due to the fact that the permanent magnets could reach the magnet's Curie temperature and thus lose its magnetism, which could damage the sputtering gun. Figure 3.5 shows the sputtering gun (model Onyx-2 DC Std Angstrom Sciences, Inc) used. This sputtering gun needs a minimum flow rate for correct refrigeration (5gallons/minute). The water flow must be maintained for 15 minutes after power has been

turned off to sufficiently cool the cathode body and prevent the magnet from overheating.

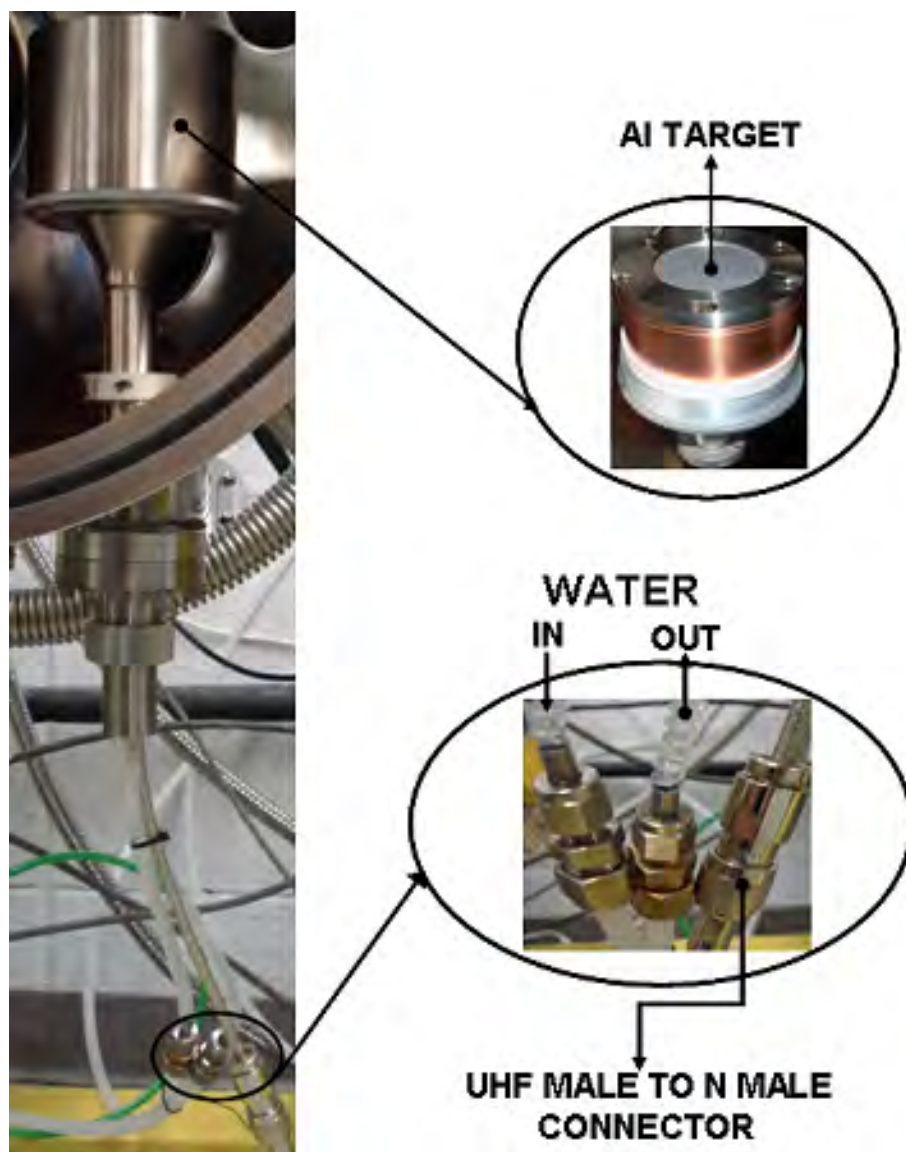


Figure 3.5: Sputtering Gun.

The refrigeration control system is fed by the output of a mechanical sensor, whose purpose is to monitor the presence and absence of a water flow. The mechanical sensor can be used as a switch by using its common open or close outputs. This switch is used to determine the presence or absence of a water flow across the sputtering gun.

The power supply of the sputtering gun needed a UHF male to N Male connector and a coaxial cable RG8 shorter than 3.05m (10') for its optimal performance.

### C) Controllers:

The PVD Controllers are shown in the Figure 3.6.

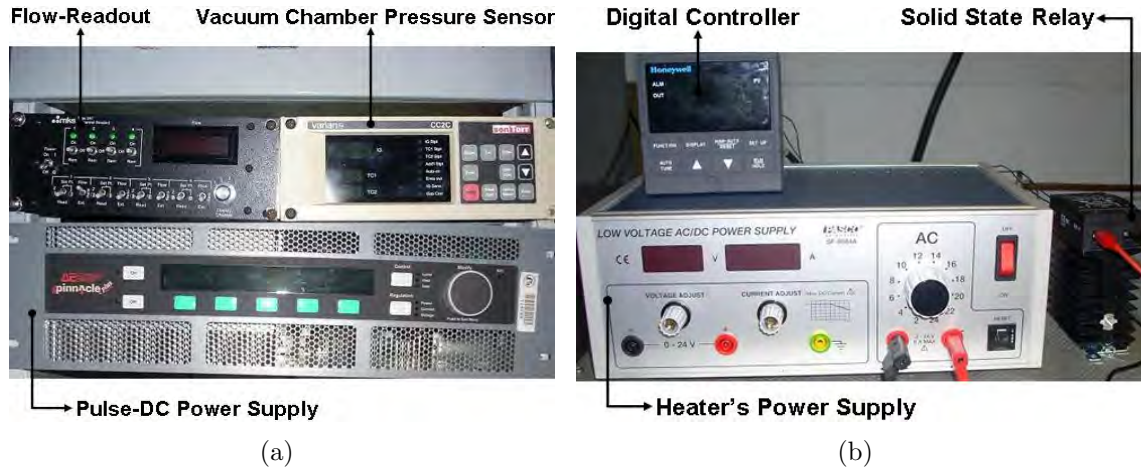


Figure 3.6: Controllers: (a) Power supply of the sputtering gun and flow-readout; (b) Temperature controller.

Figure 3.6(a) shows the power supply (Pinnacle Plus+ 5kW, Advanced Energy Industries) of the sputtering gun. This can provide up to 5kW of power and 325-650 Vdc. Figure 3.6(a) shows the readout for the two mass-flow controllers. One of them is for controller 50sccm ( $N_2$ ), whereas the other one is for 100sccm (Ar). Figure 3.6(b) shows the temperature controller used. The power supply output was limited to 6A and 10V to protect the heater. These current and voltage values were enough to reach the deposition temperature previously shown in Table 3.1.

# CHAPTER 4

## EXPERIMENTAL RESULTS

### 4.1 Introduction

The current revolution in nanotechnology has been supported with improvement of old and the introduction of new instrumentation systems for evaluating and characterizing nanostructures. Different instruments and methods are being used for the characterization of the physical, chemical, and structural properties of a particular material, each one of them with advantages and disadvantages depending on the material, compounds or solid to be studied.

For characterization of nanomaterials, the two most commonly used techniques are XRD and AFM. XRD techniques give information about the structure of solids (arrangement of the atoms that compose the solid) using nondestructive structure analyses. Some of the most important information that we could obtain from this technique were the kind and quantity of materials that compose a solid, the quantity of materials that are crystallized, and average orientation of crystallites that compose the solid. AFM is a form of scanning probe used to obtain information about the sample's surface through detection of the interatomic forces between the probe tip (very sharp tip of pyramidal or conical form) and the sample surface.

This chapter shows the deposition details of AlN thin films prepared for this work and their characterization using XRD and AFM. Three different substrates have been used for this characterization. A comparison of the results was done.

## 4.2 Deposition and Characterization of AlN thin films

The deposition of AlN was done using the sputtering system described in Chapter 3. Some of the parameters used as initial experimental conditions were shown in Table 2.2. Other parameters were changed during the experimentation.

The deposition of AlN films was done using pulsed-DC power to avoid arcing. The correct selection of the on-time pulse (charge), reverse-time pulse (discharge), and frequency parameters is very important. During all the experimentation, these parameters were left fixed and were taken from the work done by Lee and Cuomo [27] as shown in Figure 4.1. The distance between the target and substrate was fixed

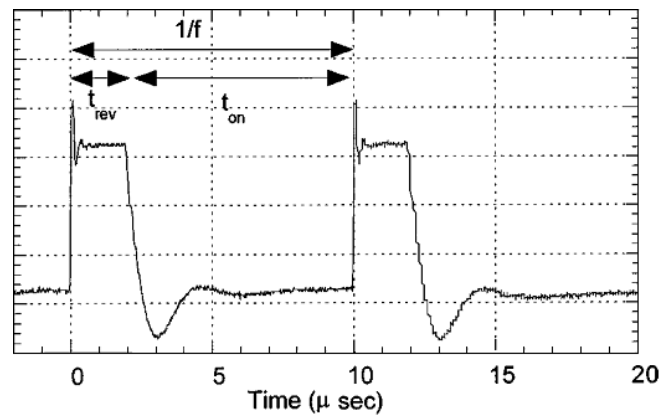


Figure 4.1: Target wave form at 100 kHz, 80% of duty cycle.

at 3.3 inches (close value to the 3 inches used by Lee and Cuomo). The deposition temperature was fixed to 500 °C (typical temperature for depositions of AlN), and parameters such as the deposition pressure and the flow ratio of N<sub>2</sub> and Ar were changed between experiments.

The Al sputtering target (99.995%) used had a diameter of 2 inches and a thickness of 0.25 inches. When the target was mounted into the circular sputtering gun (Figure 3.5) it was necessary to use the spacing tool provided by the supplier in order to ensure a space between the anode shield and the target clamping ring.

The DC power supply (Figure 3.6(a)) configuration parameters were reduced to: frequency, reverse time, and power of the target wave form.

The deposition temperature was controlled using a universal digital controller Honeywell (UDC2300), a low voltage AC/DC power supply (Pasco Scientific SF-9584A), and a solid state relay (Crydom CMRD2435). These elements were shown in Figure 3.6(b).

The flow ratio of N<sub>2</sub> and Ar was controlled using the mass flow controllers. The background pressure in the vacuum chamber was about 10<sup>-8</sup> Torr, maintained by a cryopump (APD Cryogenics Inc) and a helium compressor model HC-4 MK2 (Figure 3.2). This pressure was sensed with a vacuum gauge (Varian Inc) and displayed in a Varian senTorr model CC2C. The cryopump is cooled down (~12 K) and maintained at very low temperatures by helium expansion. This helium must be high-purity (99.995%).

To obtain the adequate deposition pressure level, it was necessary to use a manual gate valve (MDC model LGV-8000V-P-03) with a iris diaphragm. The deposition pressure was measured with a Capacitance Diaphragm Gauge (CDG). This CDG can accurately measure pressures from 0 to 1 Torr.

The samples were placed over the heater using silver paint. The first experiments were over a Si <1 1 1> substrate. Table 4.1 shows the conditions used.

Table 4.1: AlN thin film on silicon <1 1 1> substrate.

Parameter	Value
Distance between target and substrate	3.3in
Deposition temperature	500 °C
Deposition time	45min
Frequency	100kHz
Reverse time	2μseg
Power	100W
Current	0.32A
Voltage	315V
N <sub>2</sub> flow	6.0sccm
Ar flow	10.0sccm
Deposition pressure	16mTorr

In order to confirm that the film deposited was AlN, XRD analysis was performed. A Bruker D8 Discover diffractometer (Bruker AXS, Karlsruhe, Germany) was used for these measurements. Figure 4.2 shows the XRD scans for AlN over silicon <1 1 1> substrate.

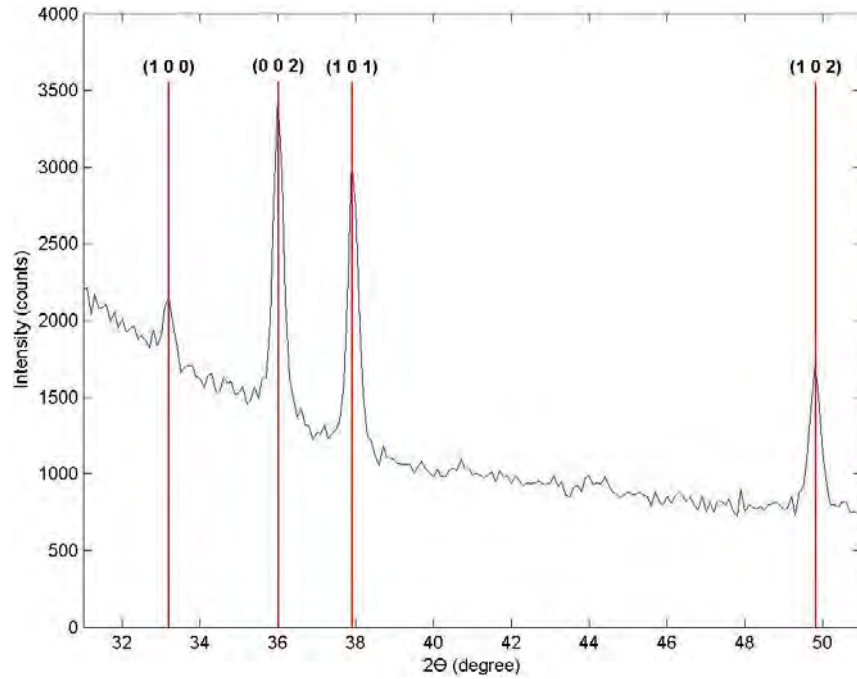


Figure 4.2: XRD with grazing angle  $3^\circ$  of AlN thin film on silicon  $\langle 1\ 1\ 1 \rangle$  substrate.

On the silicon  $\langle 1\ 1\ 1 \rangle$  substrate, the deposited AlN film shows features at around  $2\theta = 33.2^\circ$ ,  $36^\circ$ ,  $37.8^\circ$ , and  $49.8^\circ$  corresponding to the (1 0 0), (0 0 2), (1 0 1), and (1 0 2) planes of crystalline AlN, respectively.

To obtain information about the sample's surface, AFM was done using a Park Scientific Instruments CP Autoprobe. A force of 123.5nN was applied. The scanning for all images in this work were done in a window of  $2 \times 2\mu\text{m}$  and they have a magnification of 5X on the Z axis. Figure 4.3 shows the scanning image.

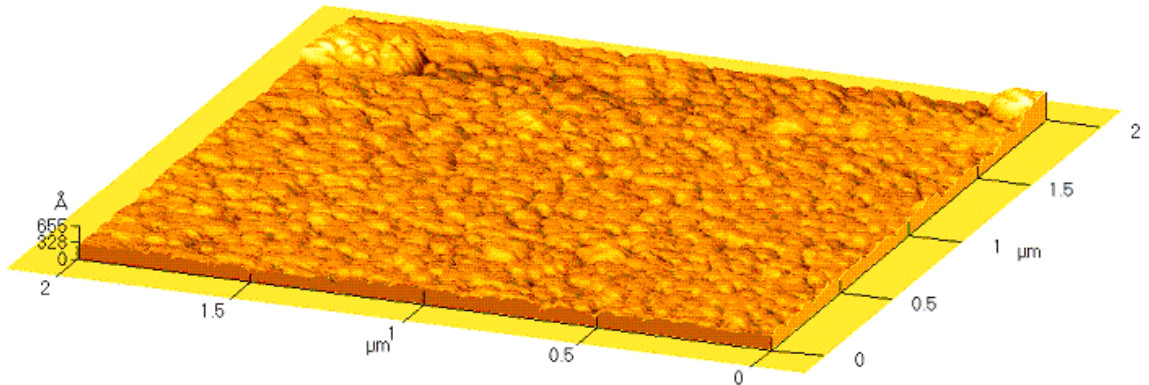


Figure 4.3: AFM of AlN thin film on silicon  $\langle 1\ 1\ 1 \rangle$  substrate.

An average grain size of 78nm and a surface roughness of 41.2Å were observed.

Increasing the deposition time from 45 to 60min, while keeping the other deposition conditions fixed (Table 4.1), an AlN film was deposited on sapphire (c-cut) substrate. Figure 4.4 shows the scans for AlN over sapphire substrate including substrate (top) and without substrate (bottom).

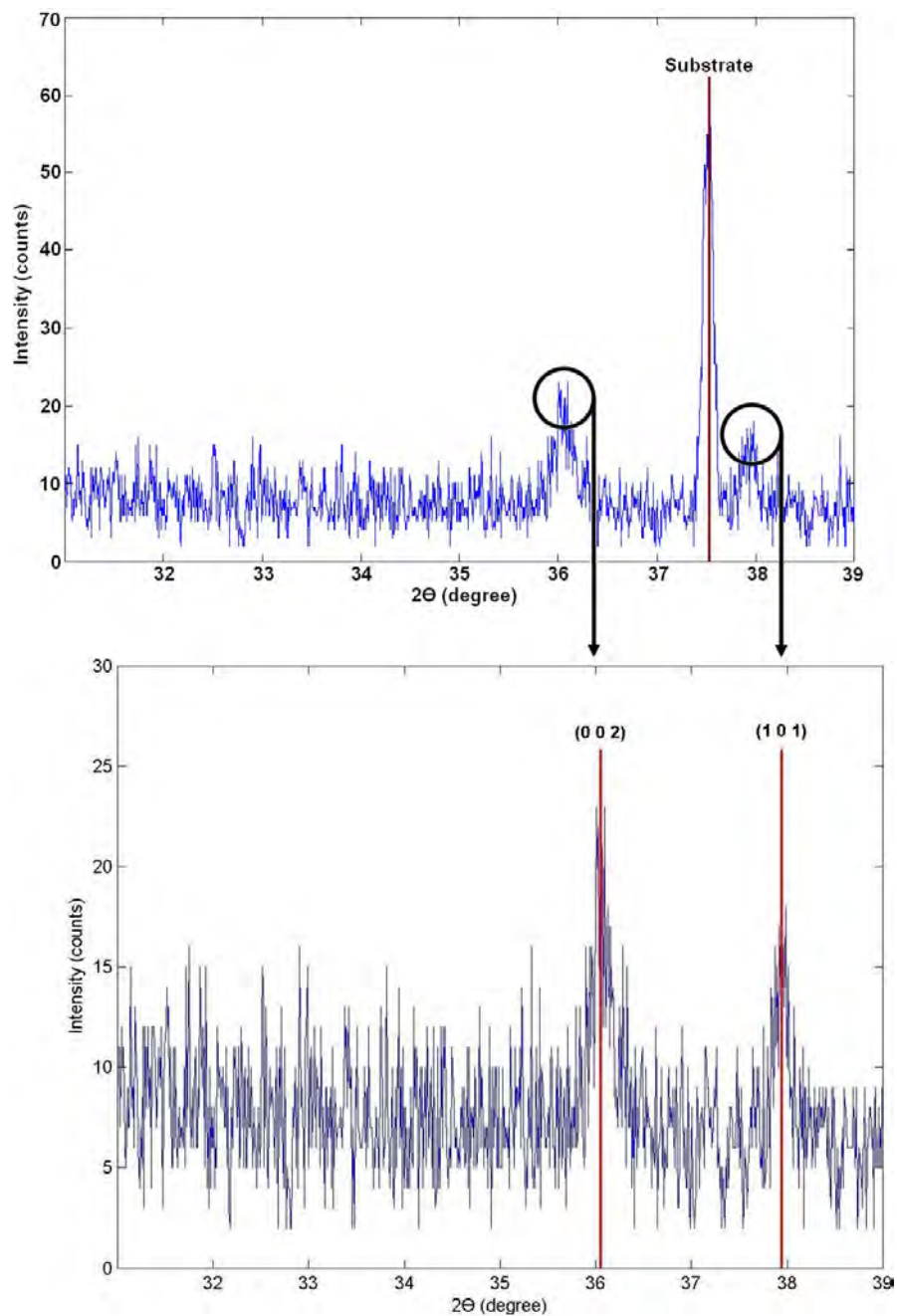


Figure 4.4: XRD of AlN thin film on sapphire (c-cut) substrate.

On the sapphire substrate, the deposited AlN film shows features in the (0 0 2) and (1 0 1) planes of crystalline AlN. This film presented partial orientation with the (0 0 1) planes, parallels to the sample surface.

Increasing the power from 100 to 115W, while keeping the other deposition conditions fixed (Table 4.1), a 450nm thick AlN film was grown on the silicon <1 0 0> substrate. Figure 4.5 shows the XRD scans for the sample including substrate (top) and without substrate (bottom).

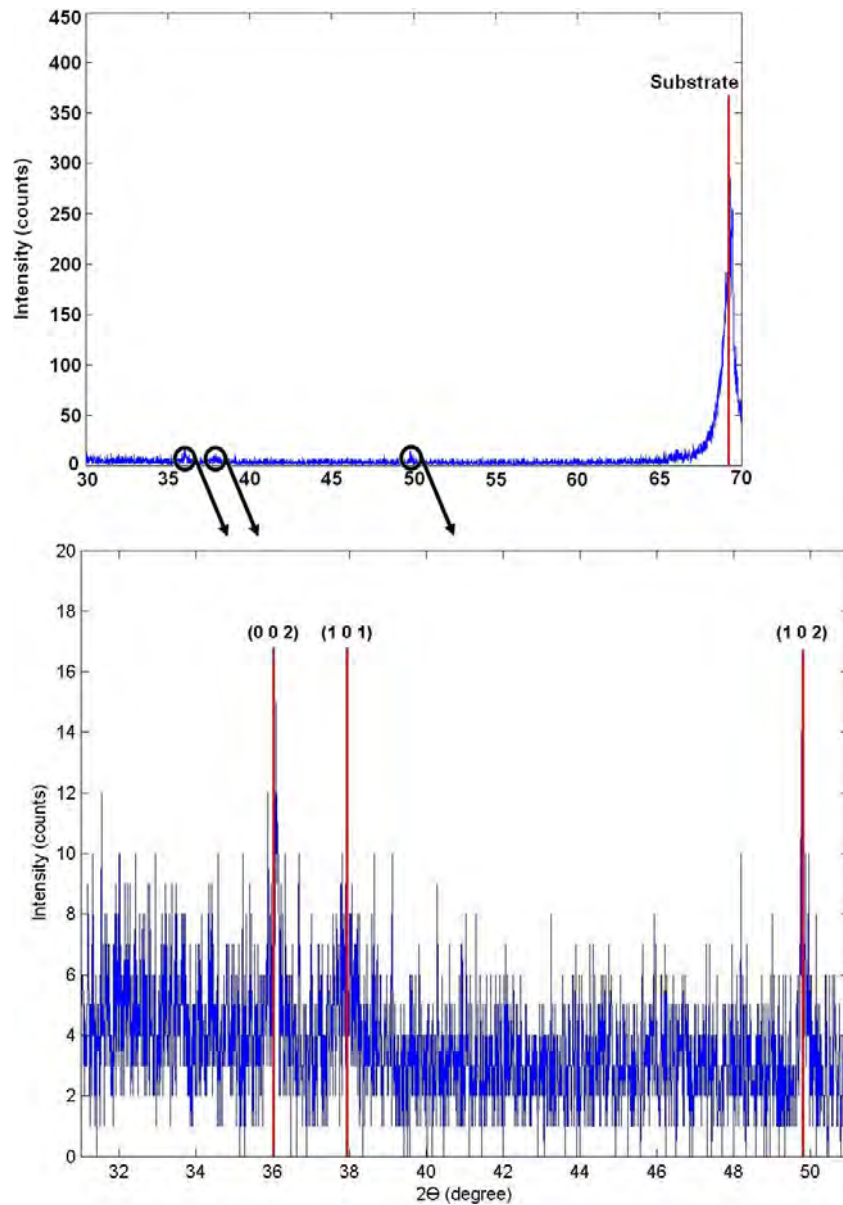


Figure 4.5: XRD of AlN thin film on silicon <1 0 0> substrate.

The thickness was measured using a profilometer (Tencor Instrument). This measurement was taken in different places on the substrate. On this silicon  $\langle 1\ 0\ 0 \rangle$  substrate, the deposited AlN film presents shows features at around  $2\theta = 36^\circ$ ,  $37.8^\circ$ , and  $49.8^\circ$  corresponding to the  $(0\ 0\ 2)$ ,  $(1\ 0\ 1)$ , and  $(1\ 0\ 2)$  planes of crystalline AlN, respectively.

AFM was performed on the sample using the same force mentioned before. Figure 4.6 shows the scanning image.

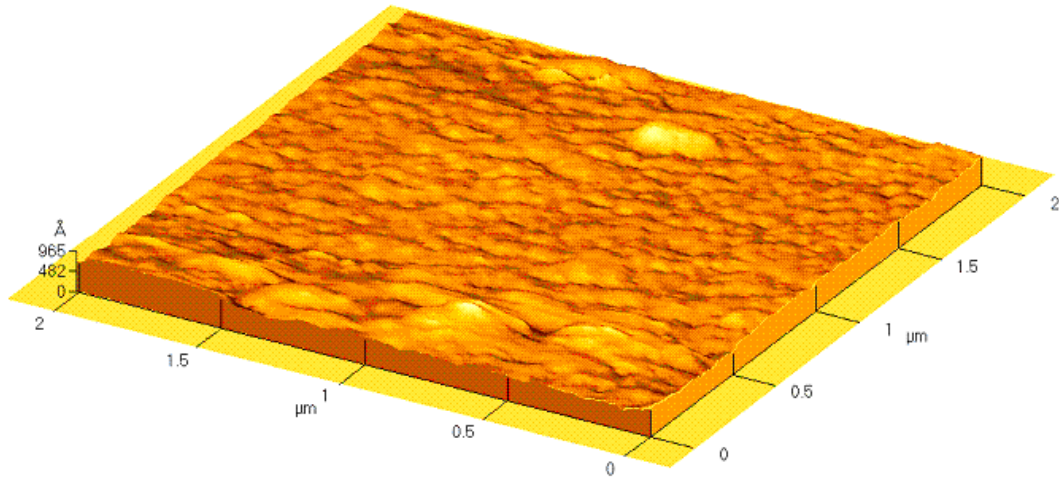


Figure 4.6: AFM of AlN thin film on silicon  $\langle 1\ 0\ 0 \rangle$  substrate.

The grain size was between 61.6nm and 268nm. An average surface roughness of  $42.4\text{\AA}$  was observed.

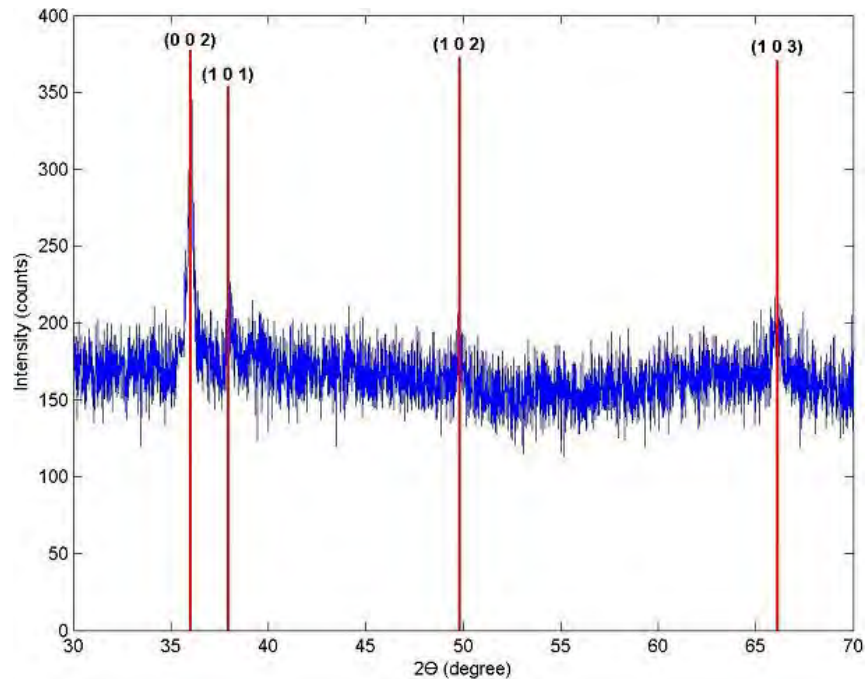
As was shown in Figures 4.2, 4.4, and 4.5, AlN films can be grown over different substrates. Nevertheless, none of the samples present an orientation preference. In some cases, this would make difficult the realization of a deep analysis of the material due to the different behavior that it could present in each direction.

In order to improve the material's orientation, the deposition pressure parameter was changed to acquire a better plasma density into the vacuum chamber. Another AlN film was deposited on a glass substrate. Table 4.2 shows the conditions used.

Table 4.2: AlN thin film on glass substrate.

Parameter	Value
Distance between target and substrate	3in
Deposition temperature	500 °C
Deposition time	45min
Frequency	100kHz
Reverse time	2 $\mu$ seg
Power	70W
Current	0.21A
Voltage	328V
N <sub>2</sub> flow	6.0sccm
Ar flow	10.0sccm
Deposition pressure	7.4mTorr

On the glass substrate, the deposited AlN film shows features at around  $2\theta = 36^\circ$ ,  $38^\circ$ ,  $49.8^\circ$ , and  $66^\circ$  corresponding to the (0 0 2), (1 0 1), (1 0 2) and (1 0 3) planes of crystalline AlN, respectively. A thickness of 170nm was measured using the profilometer. Figure 4.7 shows the scans for AlN over glass substrate.

Figure 4.7: XRD with grazing angle  $3^\circ$  of AlN thin film on glass substrate.

A new sample of silicon <1 0 0> substrate was done using the same parameters of the previous sample (Table 4.2). Figure 4.8 shows the XRD scans for this sample.

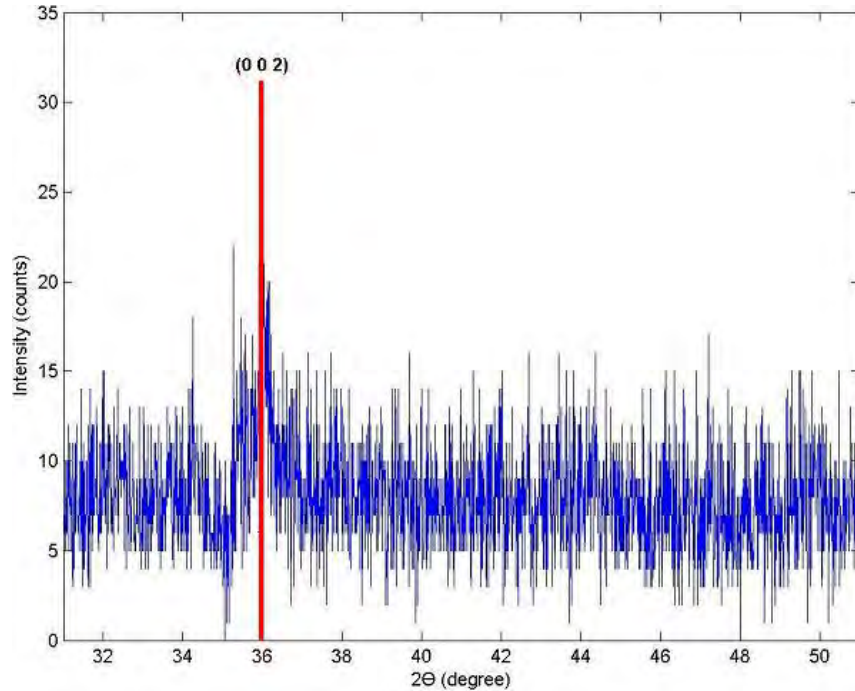


Figure 4.8: XRD of AlN thin film on silicon  $\langle 1\ 0\ 0 \rangle$  substrate.

The deposited AlN film on the silicon  $\langle 1\ 0\ 0 \rangle$  substrate shows features at around  $2\theta = 36^\circ$ , corresponding to the (0 0 2) plane of crystalline AlN. This film presented orientation with the (0 0 1) planes, parallels to the sample surface. A thickness of 280nm was measured using the profilometer and validated with an ellipsometer (J. A. Woollam Co.,Inc).

Decreasing the deposition time from 45 to 10min and keeping the other experimental conditions mentioned in Table 4.2 fixed, a 55nm thick AlN film was grown on the silicon  $\langle 1\ 0\ 0 \rangle$  substrate. This suggests a lineal behavior between deposition time and thickness in a film.

AFM analysis was done on both AlN films deposited over the silicon  $\langle 1\ 0\ 0 \rangle$  substrate. Figure 4.9 shows the AFM of the AlN film on the silicon  $\langle 1\ 0\ 0 \rangle$  with varying thickness.

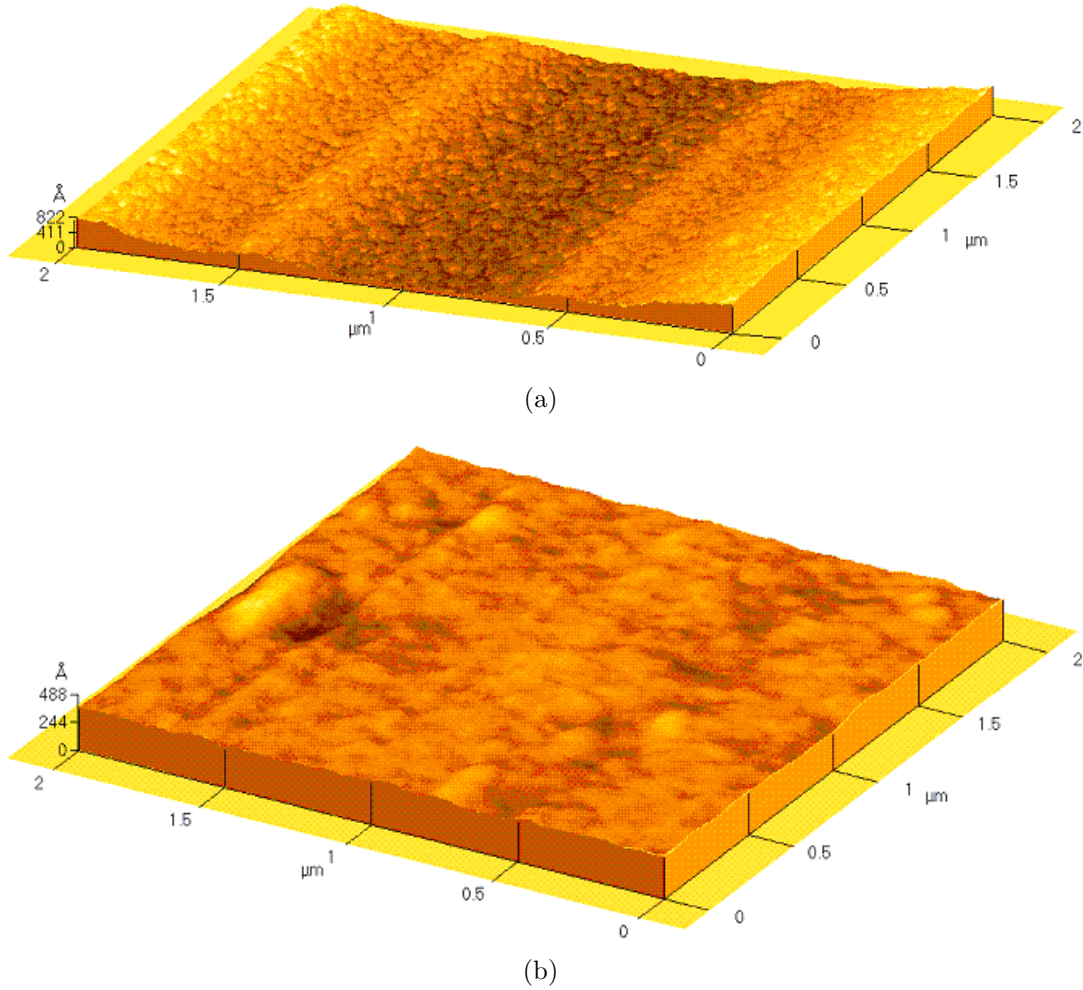


Figure 4.9: AFM of AlN thin film on silicon  $\langle 1\ 0\ 0 \rangle$  substrate: (a) 280nm of thickness; (b) 55nm of thickness.

For the 280nm thick sample, an average grain size of 40nm and a surface roughness of 129Å of average were observed. For the other sample, a grain size between 118nm and 275nm, and an average surface roughness of 18Å were observed.

### 4.3 Comparison of Results

A PVD pulsed DC sputtering system for the deposition of AlN thin films was assembled. AlN thin films were deposited in the system. Two recipes were used for the deposition over different substrates. Table 4.3 shows the two film growth parameters.

Table 4.3: AlN film growth parameters.

Parameter	Recipe 1	Recipe 2
Distance between target and substrate	3.3in	3in
Deposition temperature	500 °C	500 °C
Deposition time	60min	45min
Frequency	100kHz	100kHz
Reverse time	2 $\mu$ seg	2 $\mu$ seg
Power	100W	70W
Current	0.32A	0.21A
Voltage	315V	328V
N <sub>2</sub> flow	6.0sccm	6.0sccm
Ar flow	10.0sccm	10.0sccm
Deposition pressure	15.7mTorr	7.4mTorr

Recipe 1 was used for growth the AlN on Si  $\langle 1\ 1\ 1 \rangle$ , sapphire (c-cut), and Si  $\langle 1\ 0\ 0 \rangle$  substrates. The deposited AlN film presented partial orientation with the (0 0 1) planes, parallels to the sample surface. It is in concordance with the work presented by Meinschien et al.[31].

Recipe 2 was used for the deposition of AlN on Si  $\langle 1\ 0\ 0 \rangle$  and glass substrates. The deposited AlN film on the silicon  $\langle 1\ 0\ 0 \rangle$  substrate presented orientation with the (0 0 1) planes, parallels to the sample surface. It is in concordance with the work presented by Zhanga et al.[32] in a similar growth conditions.

The deposition rates for recipe 1 and 2 were approximately 7.5nm/min and 6.22nm/min, respectively. In recipe 2 a lower deposition rate but better film orientation than recipe 1 was observed, possibly due to the difference in deposition pressure. At low pressures, the argon plasma is more dense and causes a more energetic expulsion of the material from the target to the substrate. This helps to the film orientation, nevertheless, a lower deposition rate will be attained due to the low deposition pressure.

Recipe 1 shows grain sizes between 61.6nm and 275nm on the different substrates. The lowest grain size value was obtained using recipe 2 on a Si  $\langle 1\ 0\ 0 \rangle$  substrate with a film thickness of 280nm. There is no direct relationship between film thickness and grain size. It is in concordance with the work presented by Jergel et al.[33].

Researchers have found the surface roughness of a micromechanical resonator to influence the Q factor [34, 35]. It is therefore important to have some control over the surface roughness of AlN films which are going to be used for micromechanical resonators. In general, the AFMs show acceptable surface roughness for all samples in the different substrates used in this study.

# CHAPTER 5

## CONCLUSIONS AND FUTURE WORK

### 5.1 Conclusions

Setup of the PVD by sputtering system for deposition of aluminum nitride thin films was done. It is located in the physics building at the University of Puerto Rico - Mayaguez Campus under supervision of Dr. Felix Fernandez.

Deposition of AlN thin films over sapphire (c-cut), glass, silicon  $\langle 1\ 1\ 1 \rangle$ , and silicon  $\langle 1\ 0\ 0 \rangle$  substrates were done using the PVD by sputtering system. Two main recipes were presented. Thickness from 55nm to 450nm were grown at 500°C.

The deposition pressure was the most important parameter within the growth conditions. For a deposition pressure of 15.7mTorr, the film was deposited at a rate of 7.5nm/min. For a deposition pressure of 7.4mTorr, the deposition rate was around 6.22nm/min. From the experiments and XRD analysis, it seems that lower pressures produce more oriented AlN films.

The characterization of AlN thin films was done using XRD and AFM techniques. The results showed that AlN films deposited on sapphire substrate presented partial orientation with the (0 0 1) planes, parallel to the sample surface, while the films deposited on silicon  $\langle 1\ 0\ 0 \rangle$  substrate showed orientation with the same planes.

There is no direct relationship between thickness and grain size. Grain sizes from 61.6nm and 275nm were obtained in the AlN films on the different substrates

studied. The lowest grain size value was 40nm, and it was obtained on Si  $\langle 1\ 0\ 0 \rangle$  substrate using recipe 2.

## 5.2 Future work

The PVD sputtering system could be improved in the following way:

- During the time deposition, around 5gallons/minute of water are lost. This water is used for magnetron refrigeration. A feedback system should be implemented in order to reuse this water.
- Other magnetron could be placed into the vacuum chamber to allow film depositions of different materials without the need to break vacuum.

In order to improve the film orientation:

- Use the lowest possible deposition pressure.
- Increase the DC power during deposition.

Silicon  $\langle 1\ 0\ 0 \rangle$  substrate is commonly used to grow thin films of different materials. AlN films have been fabricated on this substrate to investigate the structural and mechanical properties of such films by Ji et al.[36]. The effect of substrate temperature on the crystal orientation and residual stress of AlN thin films were investigated on this Si  $\langle 1\ 0\ 0 \rangle$  substrate by Medjani et al.[37]. Study of AlN mechanical properties such as elastic modulus would help characterize better the AlN films. This could be obtained by measuring the resonant frequency of a coated Si cantilever beam. This study could be done using the UPRM light scattering system. Study of quality factor (Q) could be done also. A relation of the resonant frequency with: grain size, temperature, thickness, conditions of film growth, could be done.

Another techniques can be used for characterizing the structure and surface of the samples, such as X-ray Photoelectron Spectroscopy (XPS), Rutherford Backscattering Spectrometry (RBS), Scanning Capacitance Microscopy (SCM), and Scanning Electron

Microscopy (SEM) with Energy Dispersive X-ray Spectroscopy (EDS) for elemental analysis.

Aluminum nitride has been explored in the past as a new RF MEMS resonator material. The development of aluminum nitride micro and nano resonators could be done.

## REFERENCE LIST

- [1] J. Gardner.; V. Varadan.; O. Awadelkarim. *Microsensors MEMS and smart devices*. Wiley, first edition, 2001.
- [2] N. Sepulveda.; D. Aslam.; J. Sullivan. Polycrystalline Diamond MEMS resonator technology for sensor applications. *Diamond and Related Materials*, 15:398–403, 2006.
- [3] H. De Los Santos. *Introduction to Microelectromechanical Microwave Systems*. Artech House, first edition, 1999.
- [4] L. Aubin.; S. Park.; J. Huang.; H. Craighead. Microfluidic encapsulated NEMS resonators for sensor applications. In *IEEE CNF*, 2005.
- [5] A. Erbe.; G. Corso.; H. Kroemmer.; A. Kraus.; K. Richter.; R. Blick. Mechanical mixing in nonlinear nanomechanical resonators. *Applied Physics Letters*, 77:issue 19, 2000.
- [6] A. Erbe.; R. Blick. Silicon-on-insulator based nanoresonators for mechanical mixing at radio frequencies. *IEEE Transactions on Ultrasonics, Ferroelectrics, and Frequency Control*, 49:No. 8, 2002.
- [7] R. Aigner.; S. Marksteiner.; L. Elbrecht.; W. Nessler. RF-filters in mobile phone applications. *Transducers*, pages 891–894, 2003.
- [8] G. Cox.; D. Cummins.; K. Kawabe.; R. Tredgold. On the preparation, optical properties, and electrical behavior of aluminum nitride. *Journal of Physics and Chemistry of Solids*, 28:543–548, 1967.
- [9] W. Yim.; E. Stofko.; P. Zanzucchi.; J. Pankove.; M. Ettenberg.; S. Gilbert. Epitaxially grown AlN and its optical band gap. *Journal of Applied Physics*, 44:292–296, 1973.

- [10] V. Inkin.; G. Kirpilenko.; A. Kolpakov. Properties of aluminium nitride coating obtained by vacuum arc discharge method with plasma flow separation. *Diamond and Related Materials*, 10:1314–1316, 2001.
- [11] R. Farrell.; V. Pagan.; A. Kabulski.; S. Kuchibhatla.; J. Harman.; K. Kasarla.; L. Rodak.; J. Hensel.; P. Famouri.; D. Korakakis. High temperature annealing studies on the piezoelectric properties of thin aluminum nitride films. *Materials Research Society*.
- [12] L. Spina.; H. Schellevis.; N. Nenadovic.; S. Milosavljevic.; W. Wien.; A. van Herwaarden.; L. Nanver. PVD aluminium nitride as heat-spreader in IC technology. In *STW/SAFE, Veldhoven*, 2005.
- [13] L. Spina.; H. Schellevis.; L. Nanver. Aluminium Nitride layers: One way to beat the heat in silicon-on-glass technology. In *SAFE/STW, Veldhoven*, 2007.
- [14] N. Sepulveda.; D. Aslam.; J. Sullivan. Polycrystalline Diamond RF MEMS resonators with the highest quality factors. In *19th IEEE International conference on MEMS*, 2006.
- [15] G Piazza.; A. Pisano. Dry-released Post-CMOS compatible contour-mode aluminium nitride micromechanical resonators for VHF applications. Technical report, Hilton Head Workshop, 2004.
- [16] G. Piazza.; P. Stephanou.; J. Porter.; M. Wijesundara.; A. Pisano. Low motional resistance ring-shaped contour-mode aluminum nitride piezoelectric micromechanical resonators for UHF applications. *MEMS*, pages 20–23, 2005.
- [17] G. Piazza.; P. Stephanou.; A. Pisano. AlN contour-mode vibrating RF MEMS for next generation wireless communications. In *ESSDERC*, 2006.
- [18] P. Stephanou.; G. Piazza.; C. White.; M. Wijesundara.; A. Pisano. Piezoelectric thin film AlN annular dual contour mode bandpass filter. In *ASME IMECE*, 2005.

- [19] P. Stephanou.; G. Piazza.; C. White.; M. Wijesundara.; A. Pisano. Mechanically coupled contour mode piezoelectric aluminum nitride MEMS filters. *MEMS*, pages 906–909, 2006.
- [20] G. Piazza.; P. Stephanou.; A. Pisano. Piezoelectric aluminum nitride vibrating contour-mode MEMS resonators. *Journal of Microelectromechanical System*, 15:No. 6, 2006.
- [21] N. Sepulveda.; M. Toledo. Electrostatic and piezoelectric testing methods for RF MEMS resonators. In *IEEE Midwest Symposium on Circuits and Systems*, 2006.
- [22] G. Piazza.; P. Stephanou.; A. Pisano. Single-chip multiple-frequency AlN MEMS filters based on contour-mode piezoelectric resonators. *Journal of Microelectromechanical System*, 16:No. 2, 2007.
- [23] J. Jeong.; S. Chung.; S. Lee.; D. Kwon. Evaluation of elastic properties and temperature effects in Si thin films using an electrostatic microresonator. *Journal of Microelectromechanical System*, 12:No. 4, 2003.
- [24] N. Sepulveda.; A. Rua.; R. Cabrera.; F. Fernandez. Young's modulus of VO<sub>2</sub> thin films as a function of temperature including insulator-to-metal transition regime. *Applied Physics Letters*, 92:191913, 2008.
- [25] R. Bishop.; D. Johnson. *The mechanics of vibration*. Cambridge University Press, 1960.
- [26] A. Belkind.; Z. Zhao. Pulsed-DC reactive sputtering of dielectrics: Pulsing parameter effects. In *43rd Annual Technical Conference Proceedings*, 2000.
- [27] J. Lee.; J. Cuomo. Plasma characteristics in pulsed direct current reactive magnetron sputtering of aluminum nitride thin films. *Journal of Vacuum Science and Technology*, 22:260–263, 2004.
- [28] M. Nakakuki.; A. Shiono.; I. Kobayashi.; N. Tajima.; T. Yamakami. Characterization of Al-based insulating films fabricated by physical vapor deposition. *Japanese Journal of Applied Physics*, 47:609–611, 2008.

- [29] V. Mortet.; M. Nesladekb.; K. Haenenb.; A. Moreld.; M. D/Olieslaeger.; M. Vaneceka. Physical properties of polycrystalline aluminium nitride films deposited by magnetron sputtering. *Diamond and Related Materials*, 13:1120–1124, 2004.
- [30] S. Venkataraj.; D. Severin.; R. Drese.; F. Koerfer.; M. Wuttig. Structural, optical and mechanical properties of aluminium nitride films prepared by reactive dc magnetron sputtering. *Thin Solid Films*, 502:235–239, 2006.
- [31] J. Meinschien.; F. Falk.; R. Hergt.; H. Stafast. Distinct orientation of AlN thin films deposited on sapphire substrates by laser ablation. *Applied Physics: A*, 70:215218, 2000.
- [32] J. Zhanga.; H. Chenga.; Y. Chena.; A. Uddina.; Shu Yuana.; S. Gengb.; S. Zhang. Growth of AlN films on Si (100) and Si (111) substrates by reactive magnetron sputtering. *Surface and Coatings Technology*, 198:68–73, 2005.
- [33] M. Jergel.; C. Falcony.; M. Aguilar.; M. Auger.; O. Sanchez.; J. Albella. Structural, optical and mechanical properties of AlN films - effect of thickness. *Superficies y Vacio*, 16:22–27, 2003.
- [34] N. Sepulveda. *Polycrystalline Diamond RF MEMS resonator technology and characterization*. PhD thesis, Michigan State University, 2005.
- [35] K. Yasumura.; T. Stowe.; E. Chow.; T. Pfafman.; T. Kenny.; B. Stipe.; D. Rugar. Quality factors in micron- and submicron-thick cantilevers. *Journal of Microelectromechanical Systems*, 9:No.1, 2000.
- [36] X. Ji.; S. Lau.; G. Yu.; W. Zhong.; B. Tay. Structural properties and nanoindentation of AlN films by a filtered cathodic vacuum arc at low temperature. *Journal of Physics D: Applied Physics*, 37:1472–1477, 2004.
- [37] F. Medjani.; R. Sanjines.; G. Allidi.; A. Karimi. Effect of substrate temperature and bias voltage on the crystallite orientation in RF magnetron sputtered AlN thin films. *Thin Solid Films*, 515:260–265, 2006.